Microb Ecol (2013) 66:335–350
DOI 10.1007/s00248-013-0223-2

ENVIRONMENTAL MICROBIOLOGY

Diversity of Endosymbiotic *Nostoc* in *Gunnera magellanica* (L) from Tierra del Fuego, Chile

M. A. Fernández-Martínez · A. de los Ríos · L. G. Sancho · S. Pérez-Ortega

Received: 20 November 2012 / Accepted: 20 March 2013 / Published online: 23 April 2013

Abstract Global warming is causing ice retreat in glaciers worldwide, most visibly over the last few decades in some areas of the planet. One of the most affected areas is the region of Tierra del Fuego (southern South America). Vascular plant recolonisation of recently deglaciated areas in this region is initiated by *Gunnera magellanica*, which forms symbiotic associations with the cyanobacterial genus *Nostoc*, a trait that likely confers advantages in this colonisation process. This symbiotic association in the genus *Gunnera* is notable as it represents the only known symbiotic relationship between angiosperms and cyanobacteria. The aim of this work was to study the genetic diversity of the *Nostoc* symbionts in *Gunnera* at three different, nested scale levels: specimen, population and region. Three different genomic regions were examined in the study: a fragment of the small subunit ribosomal RNA gene (*16S*), the RuBisCO large subunit gene coupled with its promoter sequence and a chaperon-like protein (*rbc*LX) and the ribosomal internal transcribed spacer (ITS) region. The identity of *Nostoc* as the symbiont was confirmed in all the infected rhizome tissue analysed. Strains isolated in the present study were closely related to strains known to form symbioses with other organisms, such as lichen-forming fungi or bryophytes. We found 12 unique haplotypes in the *16S* rRNA (small subunit) region analysis, 19 unique haplotypes in the ITS region analysis and 57 in the RuBisCO proteins region (*rbc*LX). No genetic variability was found among *Nostoc* symbionts within a single host plant while *Nostoc* populations among different host plants within a given sampling site revealed major differences. Noteworthy, interpopulation variation was also shown between recently deglaciated soils and more ancient ones, between eastern and western sites and between northern and southern slopes of Cordillera Darwin. The cell structure of the symbiotic relationship was observed with low-temperature scanning electron microscopy, showing changes in morphology of both cyanobiont cells (differentiate more heterocysts) and plant cells (increased size). Developmental stages of the symbiosis, including cell walls and membranes and EPS matrix states, were also observed.

M. A. Fernández-Martínez (✉) · A. de los Ríos · S. Pérez-Ortega
Museo Nacional de Ciencias Naturales-CSIC, C/Serrano 115 bis., 28006 Madrid, Spain
e-mail: ma.fernandez@mncn.csic.es

A. de los Ríos
e-mail: arios@ccma.csic.es

S. Pérez-Ortega
e-mail: sperezortega@ccma.csic.es

L. G. Sancho
Departamento de Biología Vegetal II, Facultad de Farmacia, Universidad Complutense de Madrid, 28040 Madrid, Spain
e-mail: sancholg@farm.ucm.es

Introduction

Pioneer colonisation by microorganisms is important for the later establishment of higher organisms on newly exposed substrata [1–4]. The modification of soil conditions includes increased water retention, stabilisation of micro- and macroparticles and incorporation of nutrients such as organic carbon by photosynthesis or nitrogen by nitrogen fixation [5–7]. These processes occur in a variety of environments, including recently deglaciated areas. Glacier retreat, visible nowadays in polar and subpolar areas of both hemispheres due to global warming [8–11], exposes to the atmosphere soils and rocks previously covered by ice. The first colonisation events consist of psychrophilic microorganisms, including cyanobacteria [12, 13] that may have been present in the crust under the ice (or within the ice itself [14]) or that reach the site just after exposure [15, 16]. This is followed by colonisation of exposed rocks and soil by other organisms such as lichens or bryophytes, and finally by the

establishment of vascular plants [3, 4, 17–19]. In this process, symbioses (such as lichens, mycorrhizae or plant–bacteria symbiotic associations) play an important role, enabling or increasing the colonisation abilities of the organisms involved, mainly by means of nutrient acquisition [20]. There is a large range of plants and microorganisms able to establish symbiotic relationships (reviewed by [21–25]), including plants such as legumes or cycads [26–28] and microbes such as Proteobacteria (e.g. *Rhizobium*) and filamentous, heterocyst-forming cyanobacteria (genera *Nostoc* and *Anabaena* [29]). Of particular interest is the symbiotic relationship between the plant genus *Gunnera* (Gunneraceae) and its cyanobacterial endosymbiont, *Nostoc* spp., as it is the only documented specific association between angiosperms and cyanobacteria [29–33]. The genus *Gunnera* consists of 61 species distributed mainly in the Southern Hemisphere, with only two species present in Tierra del Fuego [34]. These plants are perennial herbs, ranging in size from 30 cm (*Gunnera magellanica*) to more than 5 m [34]. On the other hand, the genus *Nostoc* (Nostocaceae) comprises filamentous photosynthetic cyanobacteria that can form motile filaments (called hormogonia) and differentiate into atmospheric nitrogen-fixing cells (called heterocysts); these organisms can occur in a symbiotic state or free living, in both terrestrial and aquatic habitats, and show a cosmopolitan distribution [35]. The intracellular symbiosis of *Nostoc* within the host *Gunnera* and the process of infection have been extensively studied [29–31]. When the symbiosis is established, many of the vegetative *Nostoc* cells become heterocysts that fix and transfer nitrogen to the host cell [30]. The host plant in turn exports carbon to the cyanobacterial symbiont and allows the cyanobacteria to expand their ecological niche. Multiple *Nostoc* strains are known to be able to establish symbiotic associations with different *Gunnera* species [30, 36, 37]. However, it has been addressed that a single plant might be associated only with a single *Nostoc* strain [37] as a consequence of the timing and the mechanisms of the infection process.

The aims of the present study were to investigate the genetic diversity of symbiotic *Nostoc* strains associated with *G. magellanica* at different spatial scales: within the same individual host plant and within and among several populations along Tierra del Fuego (including retreated glaciers and nearby areas with well-established ecosystem). Finally, we also aimed to characterise the relationship between the symbionts.

Materials and Methods

Study Area

G. magellanica specimens were collected in nine localities along Tierra del Fuego (XII Region, Chile). Six localities were sampled in Isla Grande, corresponding to areas where the glacial ice has been retreating over a period of time [38]. One locality on Península Brunswick and two on Isla Navarino were also sampled (Table 1).

The area is dominated by a rugged landscape, with Cordillera Darwin as the most important mountain range (reaching altitudes of 2,580 m.a.s.l.); high-altitude plateaus are also present. These sites have a maritime climate along the coast, characterised by hurricane-force winds and dense cloud cover [39]. These features, combined with the influence of the Pacific Ocean and the peculiar, distinctive orography create a significant gradient of decreasing rainfall from the Atlantic towards the Pacific shore (500 mm/year max near easternmost sites 8 and 9 vs. 4,000 mm near westernmost site 5) and between north and south slope of Cordillera Darwin [40]. The average temperature is 5 °C with little seasonal changes near the seaside [41–44].

Maps and geographic representation were carried out using the software DIVA-GIS and the information from its webpage [45].

Biological Material

G. magellanica (Gunneraceae) is an herbaceous plant species present only in the southernmost region of the Southern Hemisphere. It is a perennial diploid ($2n=34$) plant that can be monoecious or dioecious, being much smaller in size compared with other species of the genus, which is mainly tropical. Diminutive size may represent an adaptation to more challenging environments [34]. Cyanobacteria-infected regions ($n=181$) inside the rhizome of complete *G. magellanica* specimens ($n=133$) were collected and stored individually at −20 °C (samples from sites 1–7), while the samples from sites 8 and 9 were immersed in cetyltrimethylammonium bromide (CTAB) buffer [46], and transported to the laboratory.

From each plant, at least one symbiotic colony was extracted in aseptic conditions, avoiding as much as possible the inclusion of surrounding vegetal tissue, as well as fragments of non-cyanobacteria-infected rhizome tissue from four different specimens used as negative controls. The DNA extraction was carried out according to Cubero et al. [46], with a modification at the lysis step, extending it to a 12-h length.

PCR Amplification and Sequencing

Three different regions from the cyanobacterial genome were amplified: a fragment of the 16S ribosomal RNA gene (*16S*); the 16S–23S internal transcribed spacer (ITS); and the RuBisCO large subunit gene coupled with its promoter sequence and chaperon-like proteins (*rbc*LX). Reaction mix was carried out following O'Brien et al. [47], completing a

Table 1 Collecting data for each of the localities studied

Site	Latitude	Longitude	No. of specimens	Collector	Date of collection
Site 1: Isla Grande de Tierra del Fuego. Bahía Ainsworth	S 54°29′10.1″	W 69°36′52.4″	12	S. Pérez-Ortega	January 2010
Site 2: Isla Grande de Tierra del Fuego. Bahía Fitton	S 54°25′55″	W 70°7′48″	15	S. Pérez-Ortega	January 2010
Site 3: Isla Grande de Tierra del Fuego. Seno Agostini	S 54°24′12″	W 70°26′24″	13	S. Pérez-Ortega	January 2010
Site 4: Isla Grande de Tierra del Fuego. Glaciar Pía 1	S 54°42′36″	W 69°42′1″	14	S. Pérez-Ortega	January 2010
Site 5: Península Brunswick	S 53°50′46″	W 71°7′0″	13	S. Pérez-Ortega	January 2010
Site 6: Isla Grande de Tierra del Fuego. Bahía Parry	S 54°46′43″	W 69°42′1″	12	S. Pérez-Ortega	January 2010
Site 7: Isla Grande de Tierra del Fuego. Glaciar Pía 2	S 54°34′11.6″	W 69°8′6.32″	10	S. Pérez-Ortega	January 2010
Site 8: Isla Navarino. Nothofagus forest	S 54°56′55.97″	W 67°38′23.40″	14	M. Arróniz-Crespo	January 2010
Site 9: Isla Navarino. Cerro Bandera tundra	S 54°57′57.69″	W 67°38′21.79″	10 (7 for *rbc*LX)	M. Arróniz-Crespo	January 2010

25-μl final volume, consisting of: dNTPs (0.2 mM of each), 1.5 mM of $MgCl_2$, 0.625 units of TaqPolimerase (1 unit·μl^{-1} BioTools, Madrid, Spain), 25 μg of BSA, 0.5 μM primers (forward and reverse) and 1× PCR buffer. The cyanobacterial specific primer pair CX-CW [48] was used for the amplification of the *rbc*LX, using the following thermocycle conditions: a first 4-min step at 94 °C followed by 36 cycles of three steps: 94 °C for 30 s, 55 °C for 30 s, 72 °C for 2 min, and a final step of 72 °C for 7 min. The *16S* and ITS sequences were amplified jointly using the primer pair 359F [49] and 373R [50], following a 'Touchdown PCR' protocol, whose conditions followed Janse et al. [51]: an initial step at 94 °C for 5 min followed by 20 cycles of three steps: 94 °C for 1 min, 62–52 °C for 1 min (descending 0.5 °C per cycle, the first being performed at 62 °C and the last at 52 °C) and 72 °C for 1.5 min; 10 cycles of other three steps (94 °C for 1 min, 52 °C for 1 min and 72 °C for 1.5 min) and a final step of 72 °C for 30 min. All PCR amplifications were carried out in either a MJ Mini Personal Thermal Cycler (BIO-RAD) or a GeneAmp PCR System 2400 (Applied Biosystems). PCR products were purified using the UltraClean PCR Clean-Up kit (MO BIO Laboratories Inc.). Both DNA directions (5′-3′/3′-5′) were sequenced, with the same primer pairs used in the amplification step, by Macrogen Inc. Laboratories (South Korea) through its automatic standard sequencing service, using a 3730XL DNA sequencer under required conditions by BigDye™ terminator cycle sequencing kit. DNA extracted from non-cyanobacteria-infected plant rhizome tissue could not be amplified with the primer pairs used.

Sequence Alignment, Genetic Diversity and Phylogenetic Analyses

Complementary sequences from the same specimen and DNA region were collapsed into contigs using SeqMan software (Lasergene v 7.00, DNASTAR). Approximate identifications were obtained comparing contigs against the GenBank database by means of the BLAST algorithm [52] in order to check for contaminations, using 97 % of sequence coverage and *E* value of 0.001 parameters as threshold in the searches. Alignments were made using the software ClustalW [53], implemented within BioEdit v.7.0.9 [54], being carried out for each of the three genomic regions. Furthermore, *rbc*LX sequences obtained from the *Gunnera* specimens were aligned with sequences from *Gunnera* chloroplasts retrieved from GenBank database in order to discard previously undetected plant organelle contamination. Bellerophon [55] software was used to look for possible chimeras in all the alignments. Datasets with ambiguously aligned regions (*rbc*LX gene) were treated with the software Gblocks v.0.91b [56] prior to phylogenetic analyses.

Alignments were collapsed into haplotypes with the software Collapse 1.2 (David Posada, available at http://darwin.uvigo.es/software/collapse.html). Genetic diversity measurements were computed in DnaSP v.5 [57]. The following parameters were calculated: number of polymorphic or segregating sites (*S*); total number of mutations (*Eta*); haplotype diversity (Hd) [58]; and nucleotide diversity (π) [58]. Statistical parsimony [59] was used for later generation of genealogies (haplotype networks) using TCS v.1.21 software [60]. MOTHUR v.1.21.1 [61] was employed in order to cluster the sequences into operational taxonomic unit (OTUs) for posterior phylogenetic analyses and for study of their relative abundance by the furthest-neighbour method. Mantel tests were carried out by using the Microsoft Excel software complement GenAlEx [62] to test the role of geographic distance in the genetic structure of the endosymbionts. The genetic structure of the populations of *Nostoc* associated with *G. magellanica* was checked using the analysis of molecular variance (AMOVA) [63] for *16S* and *rbc*LX genes using the software Arlequin v.3.11 [64]. In these analyses, different groups were structured, in order to find out which

factors—environmental components of the sites, approximate time of exposition after ice retreat [38, 40] or position concerning Cordillera Darwin, i.e. North vs. South slope—better explain the genetic variance in the dataset.

Phylogenetic analyses were carried out for the *16S* and *rbc*LX genes. Collapsed haplotypes were aligned by using of ClustalW [53] with the most similar sequences found in BLAST searches [52] in the GenBank database. Most likely nucleotidic substitution models for the alignments were searched by means of the software jModelTest [65] using the Akaike information criterium [66]. The general time reversible [67] +I +G was chosen for the *16S* and the *rbc*LX alignments. Maximum likelihood phylogenetic analyses [68] were then performed, estimating support for each node using bootstrapping (10,000 repetitions), by the nearest-neighbour interchange method implemented in the software MEGA 5.05 [69]. Phylogenetic analyses based on Bayesian inference [70] were carried out with Mr. Bayes software [71], performing 30 mill generations for *16S* and 17 mill for *rbc*LX.

Low-Temperature Scanning Electron Microscopy

Small pieces of vegetal tissue hosting cyanobacterial colonies were observed by low-temperature scanning electron microscopy (LTSEM) method by being mechanically fixed onto the specimen holder of a cryotransfer system (Oxford CT1500), plunged into subcooled liquid nitrogen, and then transferred to the microscope's preparation unit via an air-lock transfer device following the protocol described by de los Ríos et al. [72]. The frozen plant tissue was cryofractured in the preparation unit and transferred directly via a second air lock to the microscope cold stage, where it was etched for 2 min at −90 °C. After ice sublimation, the etched surfaces were sputter coated with gold in the preparation unit and the tissue then placed on the cold stage of the SEM chamber. Fractured surfaces were observed under a DSM 960 Zeiss SEM microscope at −135 °C.

Results

Fifteen plants from different sampling sites were used for the intra-specimen diversity study. Sixty-three sequences for each of the three genomic regions were obtained by the amplification of DNA extracted from the colonies (with at least three sequences from different colonies per plant) for the intra-specimen diversity study. The sequences obtained from different colonies within the same host specimen were identical. Further, analyses of tissue from 133 plants generated 113 sequences each for the *16S* and ITS regions and 110 for the *rbc*LX from those same specimens of *G. magellanica* that were subsequently used for the population study level. All sequences were identified as belonging to *Nostoc* through BLAST searches in GenBank. Moreover, no chimeras were found in any alignment by the Bellerophon software analysis.

Polymorphism analyses for each genomic region and for each sampling site showed different ranges of genetic diversity (Table 2). All polymorphic parameters for *16S* showed their lowest values in sites 1 and 9. ITS region presented its lowest values for every parameter in site 1. However, *rbc*LX gene region reached its lowest values for most of the polymorphic parameters in sites 2 and 9, except for haplotype diversity, which was reached in site 1. In *16S* gene analyses, highest levels for each parameter were reached in site 3.

Table 2 Analysis of symbiotic *Nostoc* sequences diversity based on three genomic regions

Parameters	Genomic regions		
	16S	ITS	*rbc*LX
General results			
No. of sequences	113	113	110
Sequence length (No. of nucleotides)	1,040	88	907 (630)
Total No. of analysed sites	1,040	80	619 (461)
Max. No. of total haplotypes	12	19	57 (32)
No. of polymorphic sites (*S*)	41 (sites 1–9/site 3)	26 (site 1/site 2)	115 (81; sites 2–9/site 3)
Total No. of mutations (Eta)	45 (sites 1–9/site 3)	33 (site 1/site 2)	152 (85; sites 2–9/site 3)
Haplotypes			
Haplotype diversity (Hd)	0.787±0.02 (sites 1–9/site 3)	0.841±0.017 (site 1/site 5)	0.920±0.017 (0.867±0.018; site 1/site 5)
Nucleotides			
Diversity (π)	0.01606 (sites 1–9/site 3)	0.05783 (site 1/site 2)	0.06922 (0.04753; sites 2–9/site 3)
Average No. of nucleotide differences (*k*)	16.702 (sites 1–9/site 3)	4.627 (site 1/site 2)	31.978 (21.910; sites 2–9/site 3)

For *rbc*LX, after-Gblocks results appear between parentheses. Sampling sites with the lowest and the highest values appear between brackets for all genomic regions

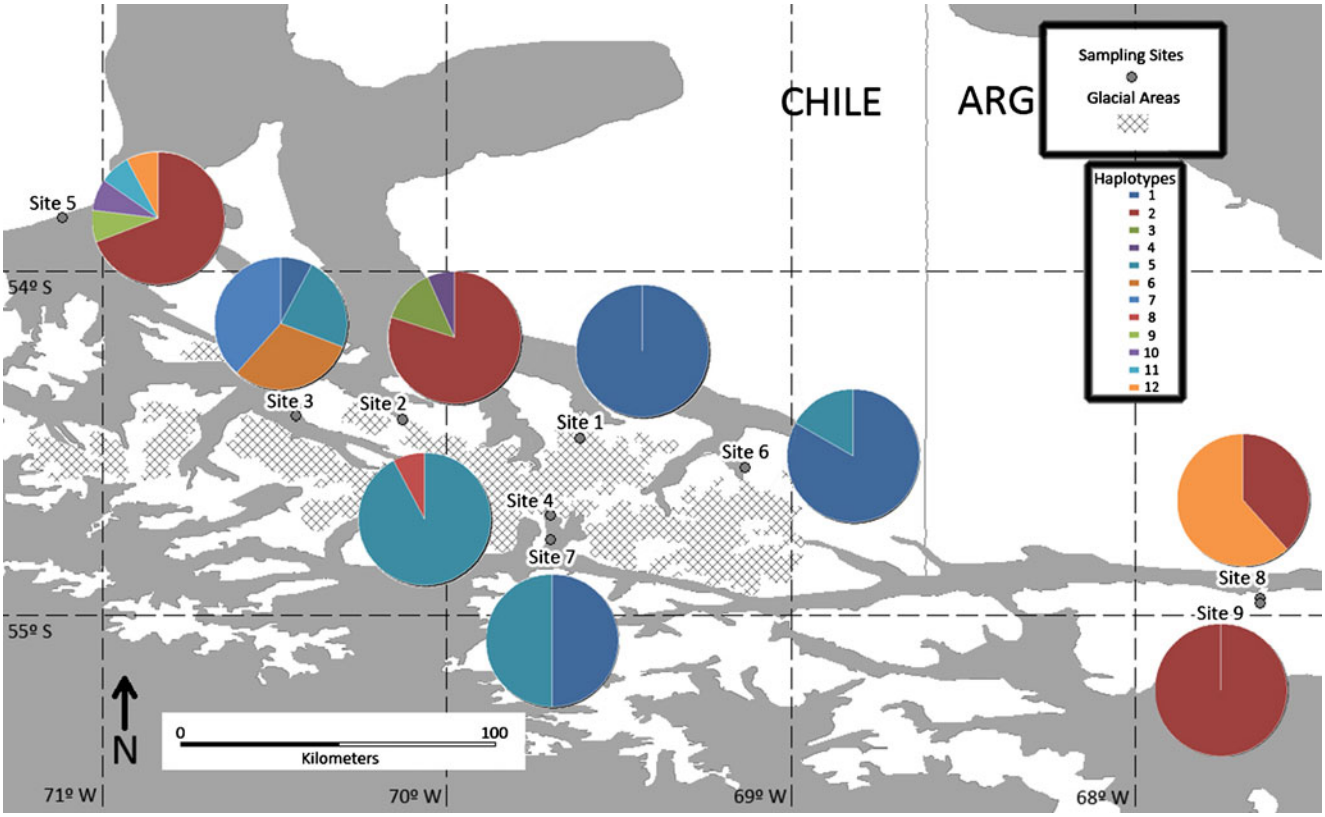

Fig. 1 Map of sampling area showing haplotypic diversity in different sites and relative abundance of each haplotype for *16S* gene data

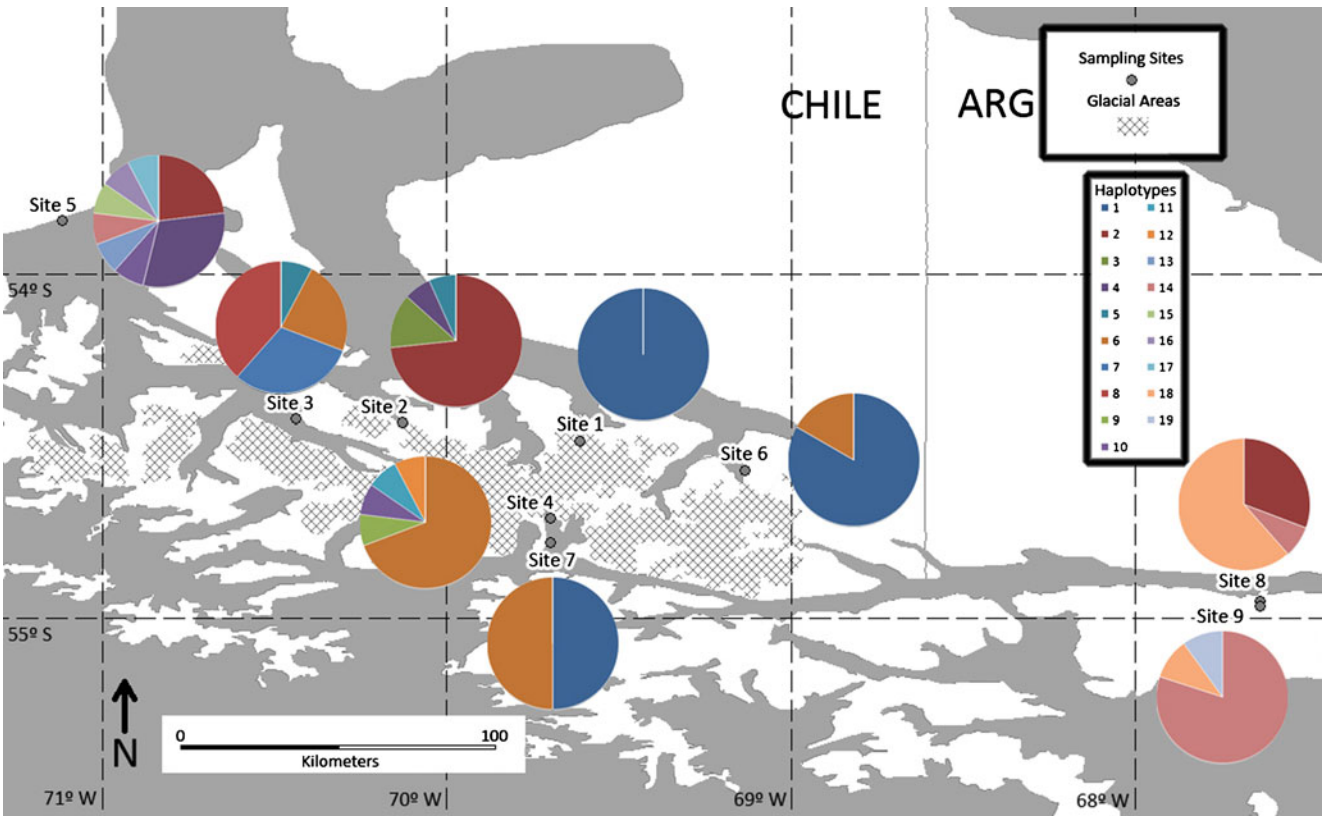

Fig. 2 Map of sampling area showing haplotypic diversity in different sites and relative abundance of each haplotype for ITS genomic region data

Parameters for ITS chromosomal region reached these maximum values in site 2 and for *rbc*LX gene in site 3, but for haplotype diversity, which reached its maximum value in site 5 for both regions.

Haplotypes found in each site and their relative abundance for *16S*, ITS and *rbc*LX regions are shown in Figs. 1, 2 and 3, respectively. For the *16S* gene, the lowest diversity was found in sites 1 and 9 with only one haplotype, followed by sites 6 and 7 with two. The greatest diversity was found in site 5 (five haplotypes). Except for sites 7 and 3, the rest of sites showed a predominant haplotype (Fig. 1). Most of the haplotypes seem to be fixed; eight of them occurred in only at a single locality. On the other hand, haplotype 12 (present in two sites) and haplotypes 1, 2 and 5 (present in four sites) showed a broader distribution.

For the ITS region, only site 1 showed one unique haplotype, whereas the rest showed at least two (Fig. 2). Site 5 showed the highest diversity with eight haplotypes. All sampling sites showed a predominant haplotype except for sites 7 and 3, represented by two equally abundant haplotypes. The broadest distribution corresponded to haplotypes number 1 and 6 (occurring in four sites), followed by 2 and 14 (three sites) and 4, 10 and 18 (two sites).

Regarding the *rbc*LX region, all sites showed more than one haplotype (Fig. 3). Site 9 showed the lowest number of haplotypes (two), while site 5 showed the highest genetic diversity with 12 haplotypes. Every site had an haplotype with more sequences than the others within it, except for sites 1 and 6, which showed two and three respectively with the same number. Haplotypes number 2 and 11 showed the broadest distribution, being present in four sites; haplotype 31 occurred in three sites, and the rest occurred only in one site.

Figure 4 shows how unique haplotypes are related by statistical parsimony, and their distribution among sampling sites, for the sequences of genomic *16S* gene (A) and ITS (B) regions. Two unconnected groups under a 95 % parsimony criterion [59] were found in the haplotypes of the *16S* ribosomal gene (Fig. 4a). The first includes 59 sequences in four haplotypes (I, II, III and IV), while the second includes the other 44 sequences in 8 haplotypes (V, VI, VII, VIII, IX, X, XI and XII). On the other hand, haplotypes from the ITS region were included in five different groups in the network analysis (Fig. 4b). Three of them (xvii, xviii and xix with 5, 1 and 2 sequences, respectively) were shown to be completely separated from the rest, two (xv and xvi with 11 sequences) were only related to each other, while the fourteen remaining haplotypes (67 sequences) showed connection under this probability criterion.

For the *16S* gene, at the level of 3 % dissimilarity (indicating putatively distinct species) 2 OTUs were

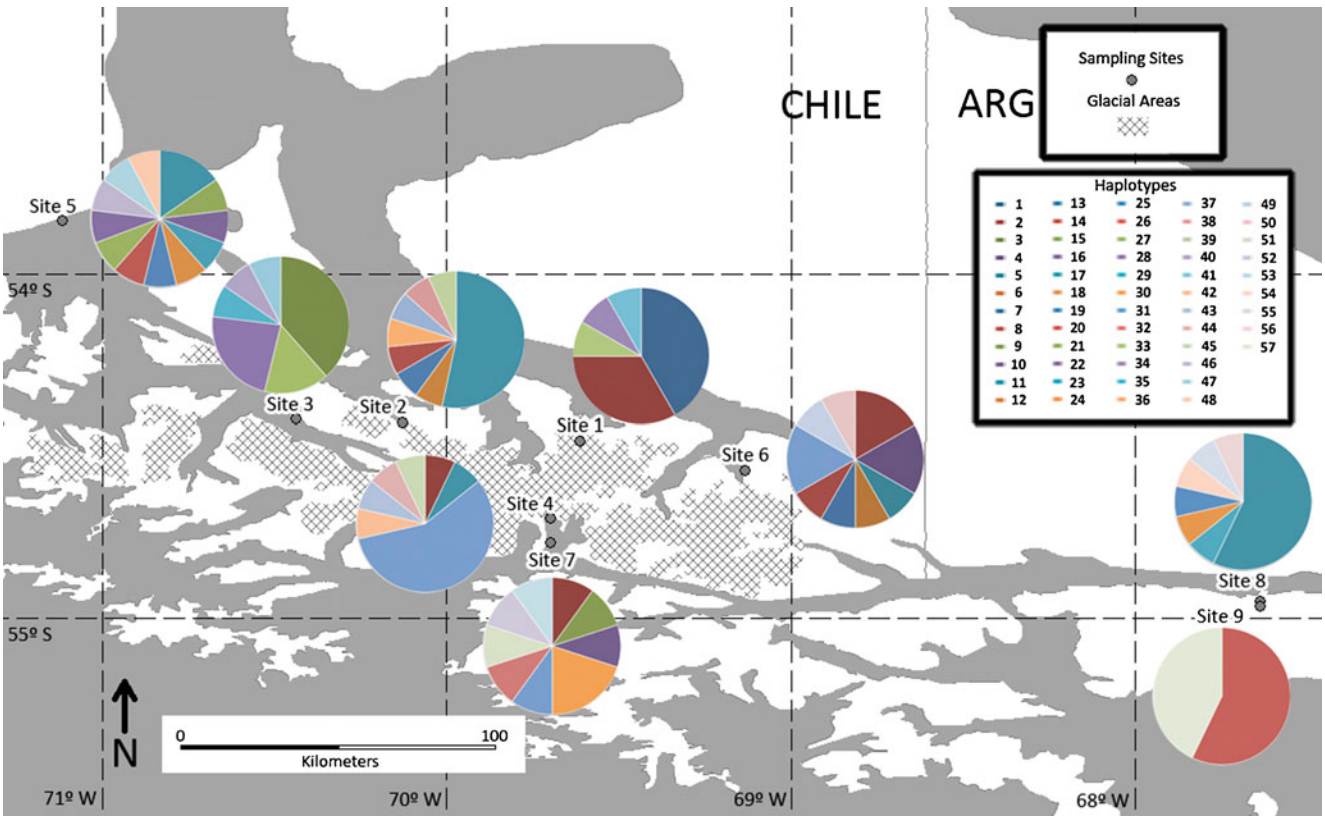

Fig. 3 Map of sampling area showing haplotypic diversity in different sites and relative abundance of each haplotype for *rbc*LX gene data

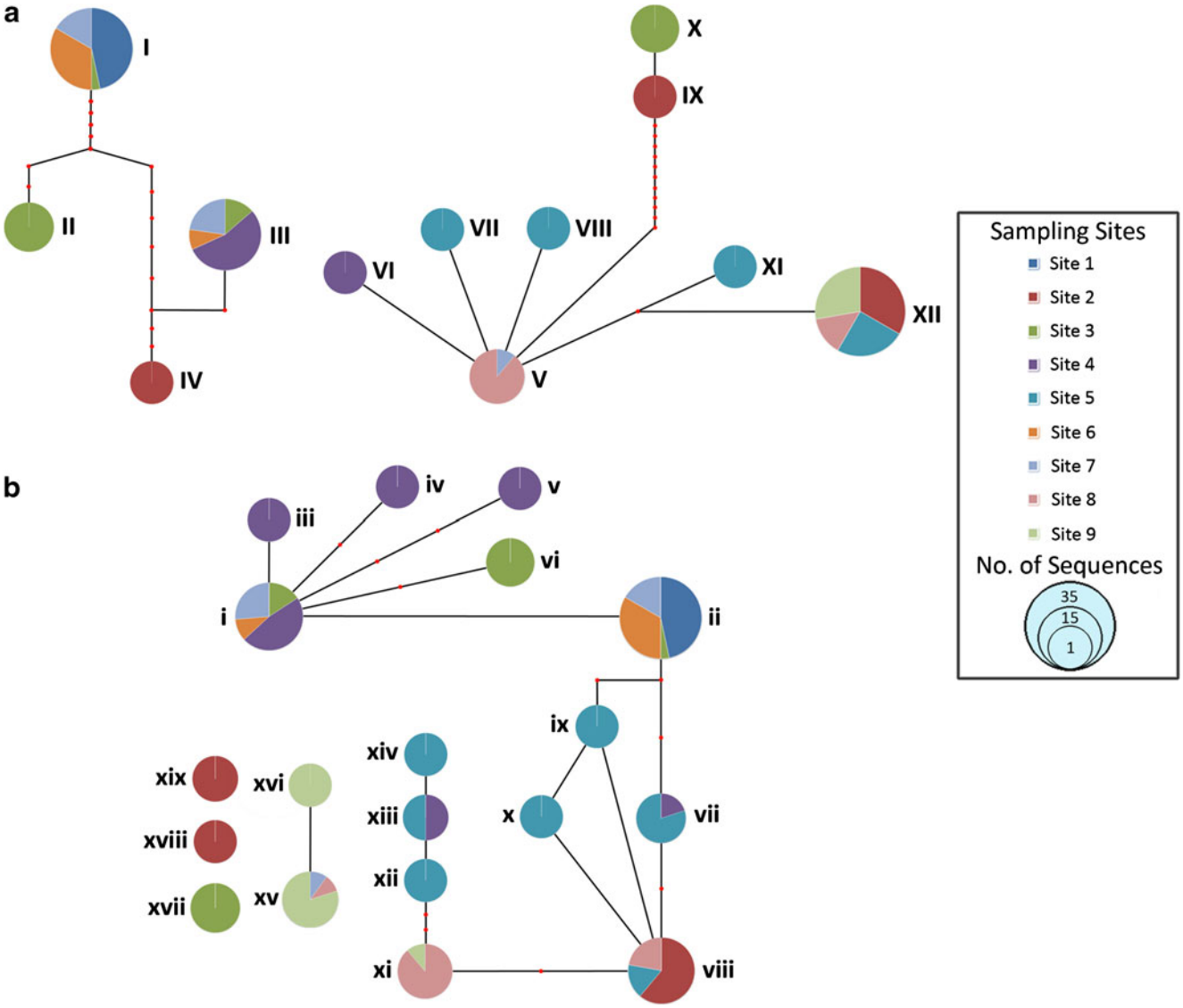

Fig. 4 Statistical parsimony networks depicting relationships among analysed haplotypes. Each *circle* represents one haplotype, and its surface area is directly related with the number of sequences integrated in it. *Roman numerals* refer to posterior comments. *Red dots along branch lines* represent the number of nucleotide substitutions between two haplotypes. **a** Haplotypes found in the sequences of *16S* gene dataset. **b** Haplotypes found in the sequences of ITS genomic region dataset

found, while at 5 % dissimilarity (indicating congeneric taxa) a single grouping was observed (Table 3). The ITS region showed 12 OTUs while the *rbc*LX gene presented 23 OTUs (6 after Gblocks trimming), using 3 % sequence dissimilarity. For the 5 % cut-off value, the number of OTUs was reduced to 8 for ITS and to 15 (4 after trimming) for *rbc*LX. Only at 20 % dissimilarity for ITS and at 18 % (8 % if Gblocks trimming is applied) for the *rbc*LX gene could 2 OTUs be recognised. These two OTUs included the same specimens independently of the analysed genomic region.

The haplotype distribution through the sampling area could reflect different environmental gradients. Figure 5 shows the response of Hd values with respect to three environmental factors. Figure 5a shows a clear trend of Hd increasing with longitude rise of the sampling areas for the three genomic regions, although low r^2's and no significant p values were found in all the cases. Evolution of Hd values for the three genomic regions in relation to time since ice retreat (Fig. 5b) and slope in the Cordillera Darwin (Fig. 5c) are also represented. Figure 5b shows there is a trend of higher Hd values in areas of longer times since deglaciation, while in Fig. 5c higher Hd values correspond to northern sites. A Mantel test showed relatively low correlation between geographic and genetic distances (0.125, p value< 0.01). Position concerning Cordillera Darwin was revealed as the most determining within the factors analysed, with percentages of 92.5 and of 63.05 of variance explained

Table 3 Number of OTUs and the number of sequences in the most common OTU obtained under different dissimilarity cut-off levels

OTUs	Genomic region		
% cut-off value	*16S*	ITS	*rbc*LX
Number of OTUs			
Unique	12	19	57 (32)
1 %	4	19	38 (13)
2 %	2	14	28 (7)
3 %	2	12	23 (6)
5 %	1	8	15 (4)
Number of sequences in the most common OTU			
Unique	36	30	22 (28)
1 %	49	30	25 (39)
2 %	59	49	28 (47)
3 %	59	50	30 (50)
5 %	113	55	30 (50)

For *rbc*LX , after-Gblocks results appear between parentheses

(p value<0.01) through AMOVA analyses for *16S* and for *rbc*LX gene regions, respectively (Table 4, North vs. South location). Other factors considered, such as the location of sampling site in retreating glacier areas and the time since ice retreated, were less explicative through independent factor analyses (Table 4).

The *16S* phylogenetic tree showed haplotypes clustered into four different groups (Fig. 6). All these groups were relatively close to sequences of different known species retrieved from the GenBank database in BLAST searches. Thus, haplotypes V, VI, VII and VIII (group I) and haplotypes XI and XII (group II) were closely related to *Nostoc edaphicum* (strain X); haplotypes I, II, III and IV (group III), together with other sequences obtained from GenBank, resulted in a group sister to *Nostoc sphaeroides* (strain HBHF0604) and finally, haplotypes IX and X (group IV) were clustered in a supported clade that includes *Nostoc flagelliforme* (strain IMGA0408). In majority of cases, the most closely related strains corresponded to sequences from

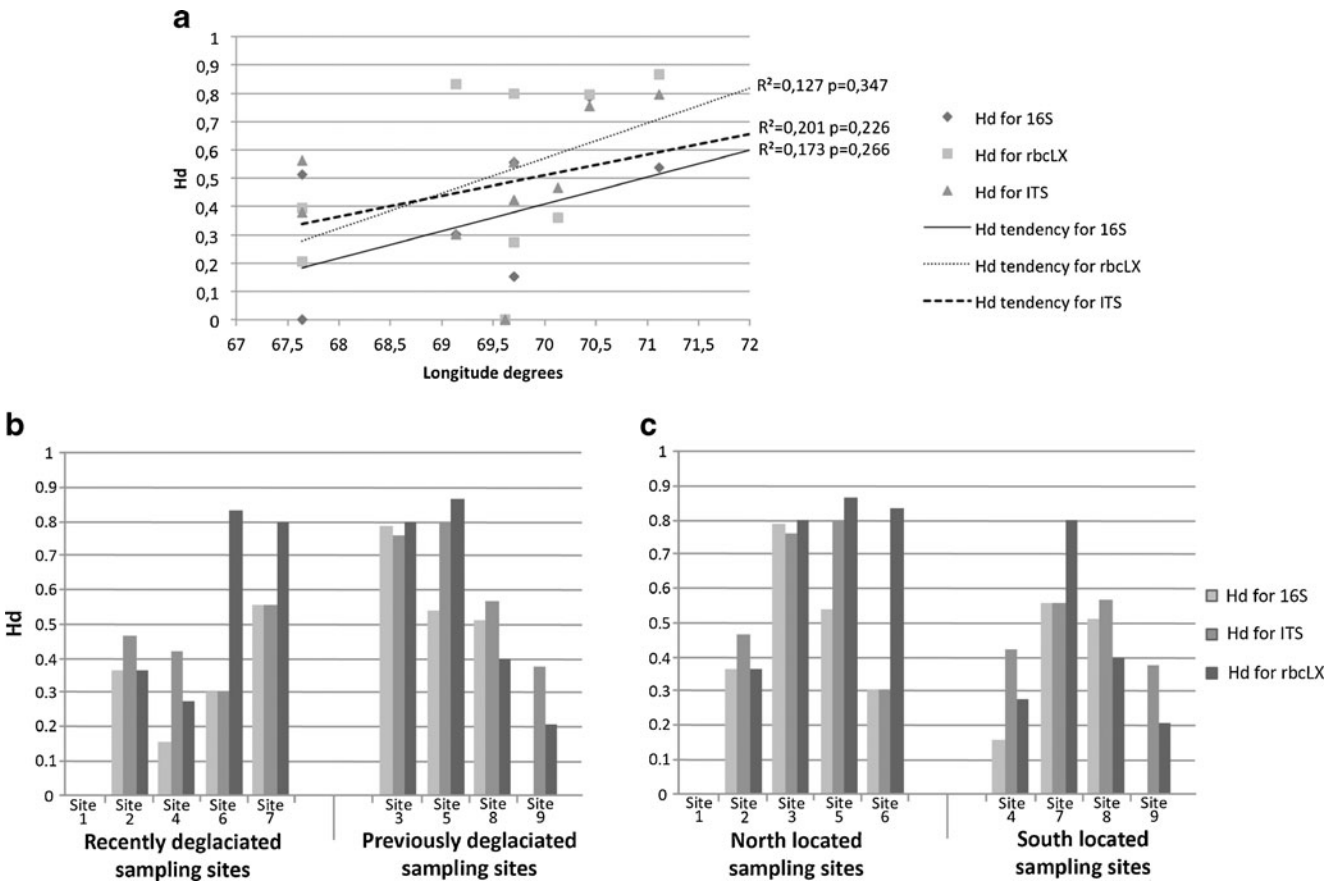

Fig. 5 Hd values for sampling sites concerning the different environmental features taken into account in present study. **a** Variation in Hd values in response to Longitude coordinate of sampling sites. Hd values are represented for the three genomic regions: *diamonds* for *16S* values and *solid line* for *16S* tendency; *squares* for *rbc*LX values and *dotted line* for *rbc*LX tendency; and *triangles* for ITS values and *discontinuous line* for ITS tendency. **b** Hd values for sampling sites, split into two groups showing sites in recently deglaciated areas (*left*) and previously deglaciated areas (*right*). Hd values are represented for the three genomic regions: *light grey* for *16S*, *grey* for ITS and *dark grey* for *rbc*LX. **c** Hd values for sampling sites, split into two groups showing northern (*left*) and southern sites (*right*). Hd values are represented for the three genomic regions: *light grey* for *16S*, *grey* for ITS and *dark grey* for *rbc*LX

Table 4 Results from AMOVA testing for *16S* and *rbc*LX genomic regions

Genomic region	Analysed parameter	Percentage of variation explained		
		Among populations	Among populations within groups	Within populations
16S	Glacier settlement	54.54 % (p=0.000)	33.02 % (p=0.118)	19.02 % (p=0.000)
	Time since ice retreat	60.90 % (p=0.000)	28.32 % (p=0.072)	21.02 % (p=0.000)
	North vs. South location	92.50 % (p=0.002)	10.69 % (p=0.619)	25.24 % (p=0.000)
*rbc*LX	Glacier settlement	49.90 % (p=0.000)	14.56 % (p=0.218)	35.54 % (p=0.000)
	Time since ice retreat	54.30 % (p=0.000)	7.81 % (p=0.208)	37.89 % (p=0.000)
	North vs. South location	63.05 % (p=0.005)	2.81 % (p=0.429)	39.77 % (p=0.000)

uncultured *Nostoc* found in symbiosis with hepatics or lichen-forming cyanobacteria (bi- and tripartite lichens).

Phylogenetic analyses for *rbc*LX gene haplotypes (Fig. 7) showed that all the haplotypes were also clustered in four major groups, with 14, 10, 6 and 2 haplotypes, respectively. The four groups are closely related to *Nostoc* sequences obtained from other symbiotic associations (mainly of the cyanolichen genus *Peltigera*, especially for

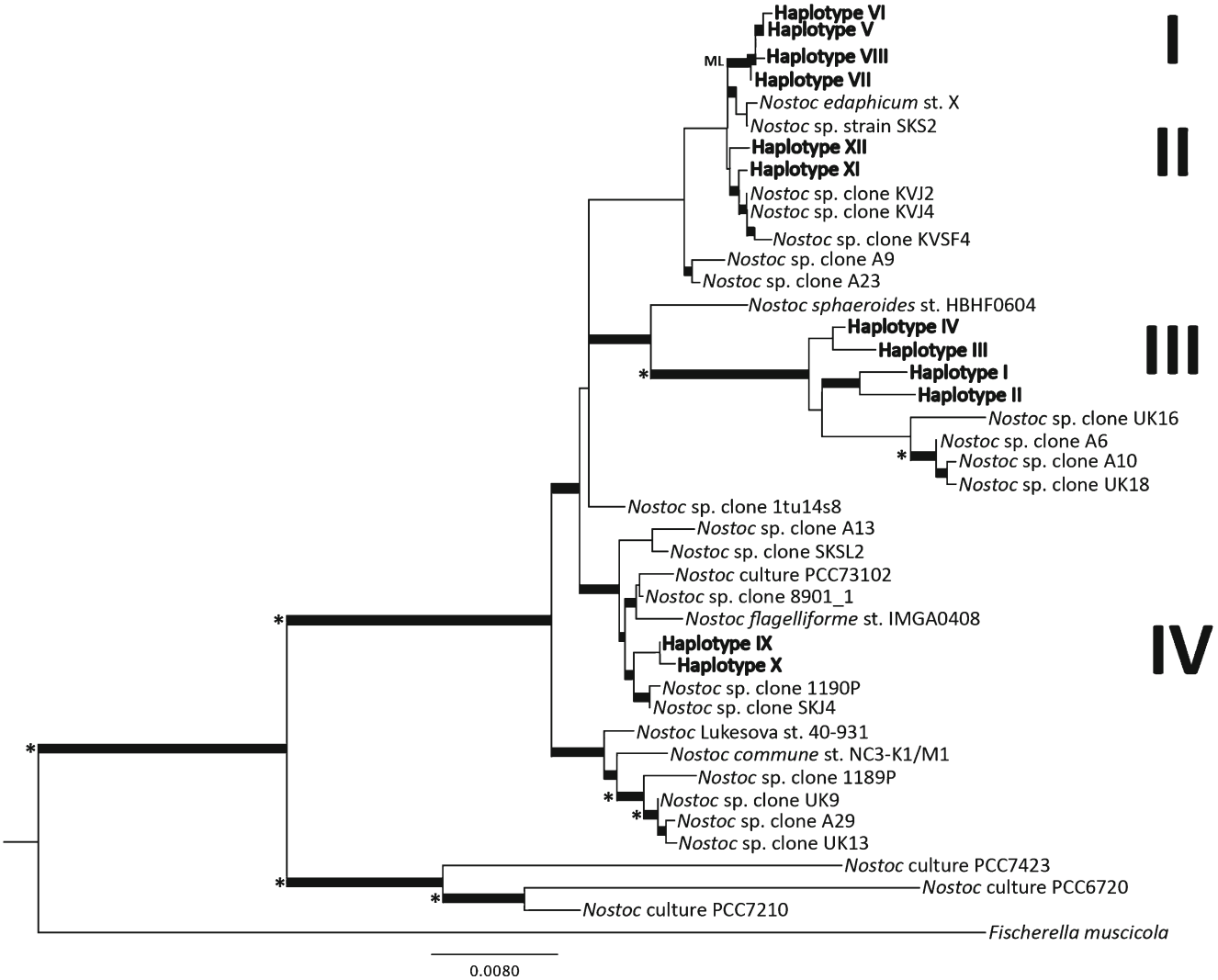

Fig. 6 Phylogenetic 50 % majority rule tree for *16S* gene dataset. *Lines in bold* show branches that are supported in Bayesian analysis (PP>0.95); those showing *ML* are supported only in maximum likelihood analysis (BP>0.70); those marked with an *asterisk* are supported in both analyses. *Line under the tree* represents substitutions per site scale. *Roman numerals* refer to posterior comments

the second and third groups). These groups could not be easily assimilated within known *Nostoc* taxa. The first and second groups seem to be close to *Nostoc* known from lichen symbioses; the third group is also close to a symbiotic *Nostoc* from a lichen, but in this case to the photobiont of *Massalongia carnosa*, which appears far from the others in the analysis. Finally, the fourth group is likely close to these *Nostoc* not only from different lichens but also to *N. flagelliforme*.

◀ **Fig. 7** Phylogenetic 50 % majority rule tree for *rbc*LX gene with collapsed haplotypes/OTUs after Gblocks trimming. *Lines* in bold show branches that are supported in Bayesian analysis (PP>0.95); those showing *ML* are supported only in maximum likelihood analysis (BP>0.70); those marked with an *asterisk* are supported in both analyses. *Line under the tree* represents substitutions per site scale. 'Haplotype 1' also comprises haplotypes/OTUs 33, 34, 35, 49 and 50; 'Haplotype 2' comprises also haplotypes/OTUs 41, 52 and 53; 'Haplotype 11' comprises also haplotypes/OTUs 36, 7, 38, 46, 47, 48, 54, 55 and 56; 'Haplotype 12' also comprises haplotype/OTU 39; 'Haplotype 26' also comprises haplotype/OTU 57; 'Haplotype 27' also comprises haplotypes/OTUs 40 and 42; 'Haplotype 31' also comprises haplotypes/OTUs 43, 44, 45 and 51. *Roman numerals* are only for easier interpretation of posterior comments

The biotrophic interface between symbiotic *Nostoc* and *G. magellanica* cells was analysed by LTSEM (Fig. 8). Infected *Gunnera* cells were numerous with larger size and more rounded shape (Fig. 8a) than uninfected ones (0 in Fig. 8b). This was especially noteworthy in later stages of infection (III in Fig. 8b). Earliest stages (I in Fig. 8b) are characterised by the intracellular location of a few *Nostoc* cells in some host cells. Penetration of small *Nostoc* cells through host cell wall was detected at these stages (arrow in Fig. 8c), which may represent first steps of infection. Microsymbiont cells were generally observed positioned close to plant cell wall (arrowheads in Fig. 8c). *Nostoc* cells appeared surrounded by host plasma membrane and embedded in a matrix of extracellular polymeric substances (EPS) (asterisk in Fig. 8c). In later stages of infection (II and III in Fig. 8b), host cells appeared colonised by filaments of *Nostoc* vegetative cells with numerous heterocysts (Fig. 8d, e). These latter cells were distinguishable by their larger size and a slightly thickened cell wall. Filaments containing heterocysts appeared embedded in an EPS matrix (asterisks in Fig. 8f).

Discussion

Results showed that every *G. magellanica* endosymbiont analysed belongs to the genus *Nostoc*, but different species are involved in the *Gunnera–Nostoc* symbioses studied. This is consistent with previous studies that identified *Nostoc* as symbiont of *Gunnera* [30, 36, 73–75], including the South Chilean host species used in the present study, *G. magellanica*, and the nearby *Gunnera tinctoria* [37, 76]. However, previous studies included only a few specimens of *G. magellanica*. The extensive sampling of different colonies in the same *Gunnera* specimen and in different specimens from diverse sites provided a better perspective on symbiont diversity at different levels and also some clues about the factors influencing these diversity values. The phylogenetic position of the different *Nostoc* symbionts found in *G. magellanica* species has been analysed for the first time.

No genetic variability was detected in *Nostoc* sampled from the same host specimen of *G. magellanica* (sequences from 15 plants). Following these results, it is possible to state that each plant was likely infected by a single strain. These results agree with those obtained in different species of *Gunnera* using fingerprinting technique [37]. The lack of intraspecimen variability has also been reported for other *Nostoc* symbiotic associations, especially those formed with bryophytes or lichen-forming fungi [77, 78]. Bonnett and Silvester [76] found similar conclusions by means of *Nostoc* inoculation assays in *Gunnera* plants, suggesting further that not every strain is able to infect every plant. Nevertheless, Nilsson et al. [79] isolated more than one strain from one single infection in *Gunnera*, identifying them by using STRR-PCR fingerprinting on cultures. Thus, present results and those obtained in cited studies point at a process of selection of symbiont strains by the plant that could occur at a very early stage of the infection process. This early selection might inhibit a second infection by other strains of cyanobacteria [80].

By contrast, genetic diversity analysis showed high intra- and intersite variability of *G. magellanica Nostoc* symbionts in Tierra del Fuego, in spite of the short distance between the easternmost and the westernmost sites (c. 350 km). Our results showed a genetic diversity gradient from the most internal sampling areas (central part of Isla Grande de Tierra del Fuego) to the most external ones (areas near oceanic coast) (Figs. 1, 2 and 3). Sites with lower haplotype diversity values (coincident results for the three studied genomic regions) were those where glacier retreat occurred most recently (since the later Late Glacial period, 10 ka) [38, 81]. On the other hand, higher haplotype diversity values were found in sites close to areas where ice disappeared in earlier times (Last Glacial Maximum and first Late Glacial periods, 20–15 ka) [38, 81]. This tendency is also shown in Fig. 5b, despite uneven Hd values for different sites. Similar results were found by Nemergut et al. [82] in a glacier foreland of the Peruvian Andes. Easternmost sites 8 and 9 (located in very close forest and tundra areas) did not show high haplotype diversity values as expected from the length of time since ice retreat [81] and the presence of stable vegetation in the area [83]. The lower diversity observed at these sites might be more influenced by the low precipitation values for both sites, and the tundra environment conditions in site 9 [40]. High precipitation values may benefit the development of both *Nostoc* and *G. magellanica* because of their physiological requirements [34], and this could favour the *Nostoc* symbiotic diversity as well as hormogonia (infective filaments) development [84, 85]. This development could drive to a more intense infection processes of all competent *Nostoc* strains of the area. In fact, higher degrees of *Nostoc* diversity was indeed found in sampling sites 3, 4, 5 and 7, areas where precipitation is more abundant. This precipitation regime is due to

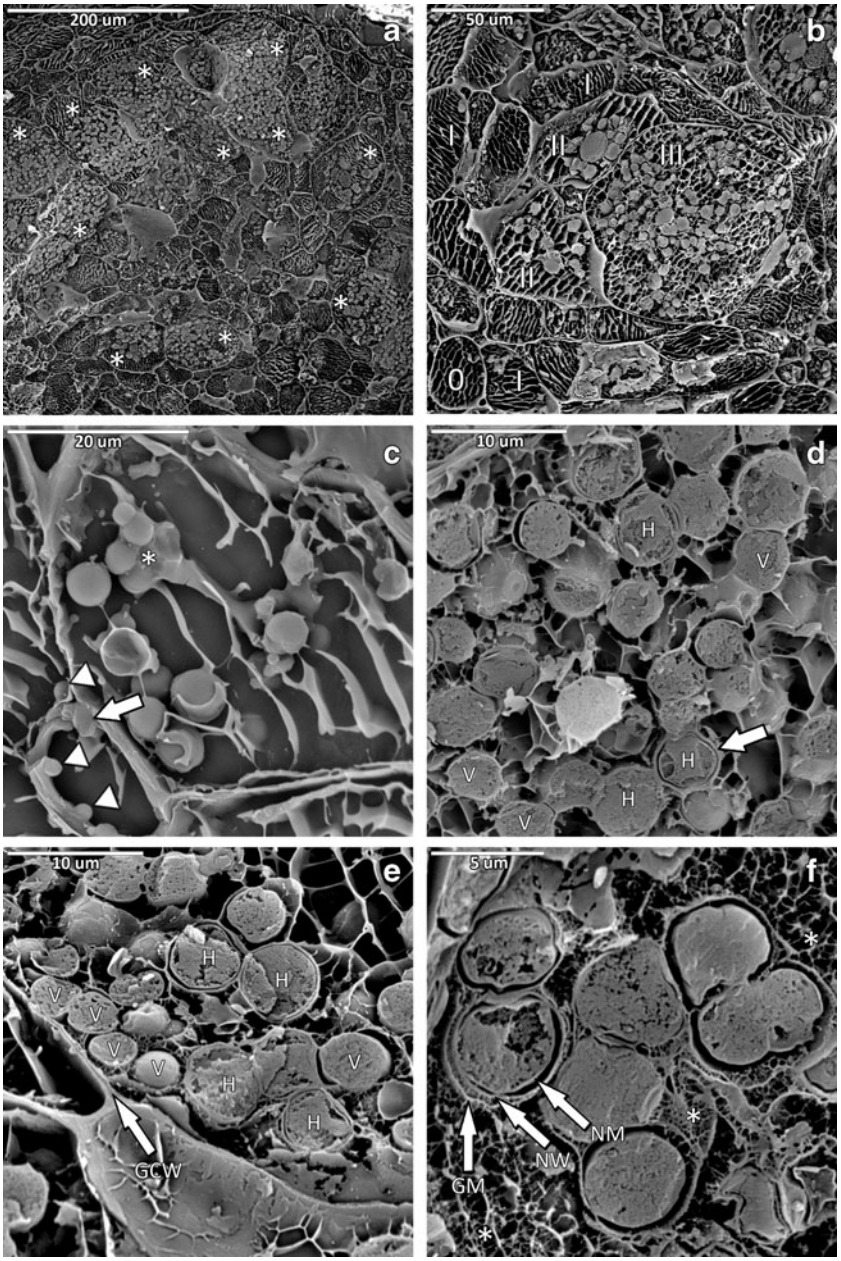

Fig. 8 LTSEM images of *G. magellanica* tissue infected with *Nostoc*. **a** Infected root tissue of *G. magellanica*; *Gunnera* cells containing *Nostoc* cells (*asterisks*) are larger than uninfected ones, also shown; **b** Area of root showing plant cells in different stages of infection by *Nostoc* cells; *0* uninfected plant cell; *I* plant cells at earliest stages of infection, with few *Nostoc* cells inside them; *II* intermediate stage of infection, with larger size and higher number of symbionts; *III* plant cell at mature infection stage, showing largest more numerous symbionts within it and with well-developed EPS matrix. **c** Infected *Gunnera* cell at an early stage of infection. *Asterisk* marks a filament of vegetative *Nostoc* cells embedded in EPS matrix. *Arrowheads* point to *Nostoc* symbiotic cells close to plant cell wall while *arrow* indicates *Nostoc* cell penetrating through host cell wall (first steps of infective processes). **d** Plant cell at a later infection stage (*III*), containing numerous filaments of *Nostoc* vegetative cells (*V*) with numerous heterocysts (*H*) distinguishable by larger size and thickened cell wall. *Arrow* points to the heterocysts cell wall showing thickness. **e** Infected host cell showing numerous *Nostoc* filaments in the proximity of its cell wall. Filaments of small vegetative cells are observed closely associated to the host cell wall (*arrowhead*). Filaments containing *H* were located inwardly. *GCW Gunnera* cell wall. **f** Detail of an infected host cell at an intermediate stage of infection (*II*), showing *Nostoc* cells bounded by host cell plasma membrane and associated with EPS fibers (*asterisks*). *Arrows* point to the three layers sourrounding *Nostoc* cell inside the host cell: *Gunnera* plasma membrane (*GM*), *Nostoc* cell wall (*NW*) and *Nostoc* membrane (*NM*)

proximity of the Pacific Ocean [38, 40] and southern exposure on a slope of Cordillera Darwin [40, 41], as well as more stable surrounding vegetation [83]. These results agree with AMOVA testing for independent factors, which showed that location with respect to the Cordillera Darwin was the factor that most explained the genetic variance

(Table 4). Moreover, low correlation between geographic and genetic distances, showed by means of a Mantel test, suggests that diversity of *Nostoc* strains associated to *G. magellanica* at each site is influenced not only by the geographic position but also by a combination of several factors.

Regarding the presence or absence of different symbiotic *Nostoc* strains in each sampling site, it is noteworthy that while some of haplotypes were present only in sampling sites furthest from the ocean (where ice-retreatment happened later), others were only shared among sites close to the ocean. This could mean that specific *Nostoc* strains might be predominant in the early stages after glacial ice retreat, as was found in analyses of *NifH* gene sequences in a retreating alpine glacier [7]. Further investigations of *Nostoc* haplotypes from soil and in symbiosis with *G. magellanica*, including Fuegian samples as close as possible to glacier ice might help to test this fact.

The finding of two OTUs by the analysis of the *16S* region of ribosomal RNA gene using a dissimilarity cut-off value of 0.03 [86–90] may indicate the presence of two distinct species. Moreover, following Hart and Sunday [91], the existence of two isolated networks of haplotypes with a 95 % parsimony probability criterion, might point to the presence of two species as well. However, four different taxa would be distinguished following the assumptions of Stackebrand and Ebers [92]: these latter authors, based on data correlation between sequence similarity and DNA-DNA reassociation experiments, considered that for prokaryotes a cut-off value of 99 % is required to discriminate between two species. In fact, phylogenetic analysis (for *16S* and also for *rbc*LX) showed that haplotypes analysed were clustered in four groups (Figs. 6 and 7). At a higher taxonomic level (using a cut-off value of 0.05, following [86, 87, 89, 90]) all the *16S* gene sequences were included in one group, indicating the presence of only the genus *Nostoc*.

The clusterings obtained by *rbc*LX sequences (without any trimming of ambiguously aligned regions) and ITS ones were equivalent to that obtained for *16S* one only when lowest cut-off values were used. The two groups resulted from *16S* sequences using a 3 % dissimilarity cut-off could also be obtained for both ITS and *rbc*LX genomic regions using cut-off values of approximately 20 % dissimilarity. Indeed, these groups for *16S*, ITS and *rbc*LX were composed of sequences obtained from the same specimens. Rudi et al. [48] found that, depending on the *Nostoc* lineage of interest, *rbc*LX region sequences divergence displays a 2- to 35-fold-higher difference compared with *16S*. With this taken into account, our results may point to the possibility of using ITS and *rbc*LX genomic regions not only for population studies [93, 94] but also for taxonomic purposes. Further analyses using a broad range of cyanobacterial groups are necessary to determine the optimum cut-off values for delimiting taxonomic groups by using sequence similarity in ITS and *rbc*LX regions, extending the criteria beyond *16S* results.

Nostoc haplotypes obtained in the present study have been shown to be closely related to *N. edaphicum*, *N. sphaeroides*, and *N. flagelliforme* by analysis of *16S* sequences. A correspondence to *N. flagelliforme* was also found in *rbc*LX analysis; this *Nostoc* species has been found before in symbiosis with other *Gunnera* species [75]. It is remarkable that many of our haplotypes showed close relationship to sequences from symbiotic *Nostoc* of different groups of organisms found in the northernmost areas of Europe. For instance, the sequences clustering with *N. edaphicum* were related to the *Nostoc* strains SKS2, KVJ2 or KVJ4, found in hepatics (retrieved from the GenBank database, not published), while those clustering with *N. flagelliforme* were related to cyanolichen symbionts from China [75].

The intracellular position of symbiotic *Nostoc* cells within *G. magellanica* has been confirmed using LTSEM. This observation was in agreement with what other authors have found using other microscopy techniques, such as TEM [95, 96]. As far as we are aware, the *Nostoc–Gunnera s*ymbiosis has not been previously examined with LTSEM. This technique allowed us to visualise the EPS matrix in which filaments of *Nostoc* cells are immersed through the infection process. Penetration of *Nostoc* cells through host cell walls and location outside the host plasma membrane could also be observed and different stages of infection characterised. The infection started with the penetration of small vegetative cells through the host cell wall (I); in later stages (II and III) filaments of *Nostoc* containing vegetative and heterocysts cells progressively occupied the entire host cell, as a host cell size increasing. All morphological and ultrastructural features were in agreement with those described in previous TEM studies [94, 95]. Further observations with this technique at different stages of host colonisation by *Nostoc* cells could increase our understanding of infection and symbiotic *Nostoc* differentiation processes.

From the results obtained in this study we conclude that an individual *G. magellanica* specimen takes up and hosts only one *Nostoc* strain. Although the *Nostoc* genetic diversity values can vary when using different markers (*16S*, ITS or *rbc*LX regions), we found a maximum of four species of *Nostoc* occurring in symbiosis with *G. magellanica* in the populations analysed. The span of time for which soils have been exposed to environmental conditions and the precipitation regime were recognised as the two prime factors influencing the values of diversity of symbiotic *Nostoc* in *G. magellanica* specimens from distinct sites in Tierra del Fuego. Through symbiosis, *Nostoc* may be extending its ecological niche sheltered from external predators. In this way, pioneer strains might persist in certain localities while new colonisations increase the diversity of *Nostoc* recognisable species by means of a dynamic process. Further studies comparing the diversity of *Nostoc* strains present in soils to those found in *Gunnera* plants are necessary to assess the degree of selectivity in this cyanobacteria–angiosperm symbiosis.

Acknowledgments The authors would like to thank Fernando Pinto (ICA, CSIC) for his technical assistance; Dr. R. Rozzi and Dr. F. Massardo and their institutions (Fundación Omora and Universidad de Magallanes) for their scientific supervision in the organisation of the field work and their logistic support. Special acknowledgment is due to Captain Mansilla and the crew of the vessel 'Don Pelegrín' for their skilful navigation in the highly demanding southern channels and for their kind hospitality on board, as well as to Dr. M. Arróniz-Crespo for her specimen collection in sites 8 and 9. Special thanks are due to Dr. W. B. Sanders for his help with English expression. This work was supported by grants CTM2009-12838-CO4-01, CTM2009-12838-CO4-03 and CTM2012-38222-C02-02 from the Spanish Ministry of Economy and Competitiveness. S. Pérez-Ortega is funded by the program JAE-Doc (Spanish Research Scientific Council) and M.A. Fernández-Martínez received funding through by the FPI program (Ministry of Economy and Competitiveness).

References

1. Matthews JA (1992) The ecology of recently deglaciated terrain. A geoecological approach to glacier forelands and primary succession. Cambridge University Press, Cambridge
2. Chapin FS III, Walker LR, Fastie CL, Sharman LC (1994) Mechanisms of primary succession following deglaciation at Glacier Bay, Alaska. Ecol Monogr 64(2):149–175
3. Hoppert M, Flies C, Günzl B, Schneider J (2004) Colonization strategies of lithobionthic microorganisms on carbonate rocks. Environ Geol 46:421–428
4. De los Ríos A, Raggio J, Pérez-Ortega S, Vivas M, Pintado A, Allan Green TG, Ascaso C, Sancho L (2011) Anatomical, morphological and ecophysiological strategies in *Placopsis pycnotheca* (lichenized fungi, Ascomycota) allowing rapid colonization of recently deglaciated soils. doi:10.1016/j.flora.2011.05.002
5. Liengen T, Olsen RA (1997) Nitrogen fixation by free-living cyanobacteria from different coastal sites in high arctic tundra, Spitsbergen. Arct Alp Res 29:470–477
6. Uliassi DD, Ruess RW (2002) Limitations to symbiotic nitrogen fixation in primary succession on the Tanana river floodplain. Ecology 83(1):88–103
7. Duc L, Noll M, Meier BE, Bürgmann H, Zeyer J (2009) High diversity of diazotrophs in the forefield of a receding Alpine glacier. Microb Ecol 57:179–190
8. Rivera A, Casassa G, Acuña C, Lange H (2000) Variaciones recientes de glaciares en Chile. Invest Geogr (Chile) 34:29–60
9. Church JA, White NJ (2006) A 20th century acceleration in global sea-level rise. Geophys Res Lett 33:L01602. doi:10.1029/2005GL024826
10. Cazenave A, Llovel W (2010) Contemporary sea level rise. Annu Rev Marine Sci 2:145–173
11. Rahmstorf S (2010) A new view on sea level rise. Nat Rep Cli Chang 4:44–45
12. Wynn-Williams DD (1996) Response of pioneer soil microalgal colonists to environmental change in Antarctica. Microb Ecol 31:177–188
13. Vincent WF (2000) Cyanobacterial dominance in the Polar Regions. In: Whitton BA, Potts M (eds) The ecology of cyanobacteria. Kluwer Academic, The Netherlands
14. Takeuchi N (2011) Glacial ecosystems. In: Singh VP, Singh P, Haritashya UK (eds) Encyclopedia of ice, snow and glaciers. Encycl Earth Sci Ser. Springer, Berlin, pp. 330–331
15. Davey MC, Rothery P (1993) Primary colonization by microalgae in relation to spatial variation in edaphic factors on Antarctic fellfield soils. J Ecol 81:335–343
16. Hodson A, Anesio AM, Tranter M, Fountain AG, Osborn M, Priscu J, Laybourn-Parry J, Sattler B (2008) Glacial ecosystems. Ecol Monogr 78:41–67
17. Grubb PJ (1986) The ecology of establishment. In: Bradshaw AD, Goode DA, Thorpe E (eds) Ecology and design in landscape. Symp Br Ecol Soc 24:83–97
18. Frenot Y, Van Vliet-Lanoë B, Gloaguen JC (1995) Particle transformation and initial soil development on a glacier foreland, Kerguelen Islands, Subantarctic. Arct Alp Res 27:107–115
19. Frenot Y, Gloaguen JC, Cannavacciuolo M, Bellido A (1998) Primary succession on glacier forelands in the Subantarctic Kerguelen Islands. J Veg Sci 9:75–84
20. Walker JR (1993) Nitrogen fixers and species replacements in primary succession. In: Miles J, Walton DWH (eds) Primary succession on land. Blackwell, Oxford
21. Stewart WDP, Rowell P, Rai AN (1980) Symbiotic nitrogen-fixing cyanobacteria. In: Stewart WDP, Gallon JR (eds) Nitrogen fixation. Academic, New York, pp 239–277
22. Stewart WDP, Rowell P, Rai AN (1983) Cyanobacteria-eukariotic plant symbiosis. Ann Microb (Instituto Pasteur) 134B:205–228
23. Smith DC, Douglas AE (1987) The biology of symbiosis. Edward Arnold, Baltimore, 302
24. Meeks JC (1998) Symbiosis between nitrogen-fixing cyanobateria and plants. BioSci 48(4):266–276
25. Bever JD, Dickie IA, Facelli E, Facelli JM, Klironomos J, Moora M, Rillig MC, Stock WD, Tibbett M, Zobel M (2010) Rooting theories of plant community ecology in microbial interactions. Trends Ecol Evol 25:468–478
26. Ow MC, Gantar M, Elhai J (1999) Reconstitution of a cycad-cyanobacterial association. Symbiosis 27:125–134
27. Costa JL, Martínez Romero E, Lindblad P (2004) Sequence based data supports a single *Nostoc* strain in individual coralloid roots of cycads. FEMS Microb Ecol 49:481–487
28. Tajhuddin N, Muralitharan G, Sundaramoorthy M, Ramamoorthy R, Ramachandran S, Abdulkadar Akbarsha M, Gunasekaran M (2010) Morphological and genetic diversity of symbiotic cyanobacteria from cycads. J Basic Microb 50:254–265
29. Rasmussen U, Johansson C, Renglin A, Petersson C, Bergman B (1996) A molecular characterization of the *Gunnera–Nostoc* symbiosis: comparison with *Rhizobium*– and *Agrobacterium*–plant interactions. New Phytol 133:391–398
30. Bergman B, Johansson C, Söderbäck E (1992) Tansley Review no. 42. The *Nostoc–Gunnera* symbiosis. New Phytol 122:379–400
31. Söderbäck E, Bergman B (1993) The *Nostoc–Gunnera* symbiosis: carbon fixation and translocation. Physiol Plant 89:125–132
32. Black K, Osborne B (2004) An assessment of photosynthethic downregulation in cyanobacteria from the *Gunnera–Nostoc* symbiosis. New Phytol 162:125–132
33. Osborne B, Bergman B (2009) Why does *Gunnera* do it and other Angiosperm don't? An evolutionary perspective on the *Gunnera–Nostoc* symbiosis. Microb Monogr 8:207–224
34. Wilkinson HP, Wanntorp L (2007) Gunneraceae. Flowering plants—Eudicots. In: The families and genera of vascular plants, vol. 9. Springer, Berlin, pp. 177–183
35. Dodds WK, Gudder DA, Mollenhauer D (1995) The ecology of *Nostoc*. J Phycol 31(1):2–18
36. Rasmussen U, Svenning MM (2001) Characterization by genotypic methods of symbiotic *Nostoc* strains isolated from five species of *Gunnera*. Arch Microb 176:204–210
37. Guevara R, Armesto JJ, Caru M (2002) Genetic diversity of *Nostoc* microsymbionts from *Gunnera tinctoria* revealed by PCR-STRR fingerprinting. Microb Ecol 44:127–136
38. Holmlund P, Fuenzalida H (1995) Anomalous glacier responses to 20th century climatic changes in Darwin Cordillera, Southern Chile. J Glaciol 41(139):465–463
39. Burgos JJ (1985) Clima del extremo sur de Sudamérica. In: Boelcke O, Moore DM, Roig FA (eds) Trans Bot Patagonia Austral. CONICET (Argentina), Royal Society (Gran Bretaña) and Instituto de la Patagonia (Chile).

40. Koppes M, Hallet B, Anderson J (2009) Synchronous acceleration of ice loss and glacial erosion, Glaciar Marinelli, Chilean Tierra del Fuego. J Glaciol 55(190):207–220
41. Capel Molina JJ (1983) Reflexiones geograficas acerca del clima frío Oceánico del Hemisferio Sur, Punta Arenas (Chile). Rev Geogr Norte Grande 10:3–16
42. Xercavins Comas A (1984) Notas sobre el clima de Magallanes (Chile). Rev Geogr 18(1):95–110
43. Endlicher W, Santana Aguila A (1988) El clima del Sur de la Patagonia y sus aspectos ecológicos. Un siglo de mediciones climatológicas en Punta Arenas. Ans Inst Pat Cs Nats, Punta Arenas (Chile) 18:57–86
44. Koremblit G, Forte Lay JA (1991) Contribución al estudio agroclimático del norte de Tierra del Fuego (Argentina). Ans Inst Pat Cs Nats, Punta Arenas (Chile) 20(1):125–134
45. Hijmans RJ, Guarino L, Cruz M, Rojas E (2001) Computer tools for spatial analysis of plant genetic resources data: 1. DIVA-GIS. Plant Genet Res Newsl 127:15–19
46. Cubero ÓF, Crespo A, Fatehi J, Bridge PD (1999) DNA extraction and PCR amplification method suitable for fresh, herbarium-stored, lichenized and other fungi. Plant Syst Evol 216:243–249
47. O'Brien HE, Miadlikowska J, Lutzoni F (2005) Assessing host specialization in symbiotic cyanobacteria associated with four closely related species of the lichen fungus Peltigera. Eur J Phycol 40:363–378
48. Rudi K, Skulberg OM, Jakobsen KS (1998) Evolution of cyanobacteria by exchange of genetic material among phyletically related strains. J Bacter 180:3453–3461
49. Nübel U, García-Pichel F, Muyzer G (1997) PCR primers to amplify rRNA genes from cyanobacteria. Appl Env Microb 63 (8):3327–3332
50. Wilmotte A, Van der Rauwera G, De Wachter R (1993) Structure of the 16-S ribosomal RNA of the thermophilic cyanobacterium chlorogloeopsis HTF ('mastigocladus laminosus HTF') strain PCC7518, and phylogenetic analysis. FEBS Lett 317:96–100
51. Janse I, Meima M, Kardinaal WEA, Zwart G (2003) High-resolution differentation of cyanobacteria by using rRNA–internal transcribed spacer denaturing gradient gel electrophoresis. Appl Env Microb 69(11):6634–6643
52. Atschul SF, Gish W, Miller W, Myers EW, Lipman DJ (1990) Basic local alignment search tool. J Mol Biol 215:403.410
53. Thompson HD, Higgins DJ, Gibson TJ (1994) CLUSTALW: improving the sensitivity of progressive multiple alignment through sequence weighting, position specific-gap penalties and weight matrix choice. Nuc Acids Res 22:4673–4680
54. Hall TA (1999) BioEdit: a user friendly biological sequence alignment editor and analysis program for Windows 95/98/NT. Nuc Acids Symp Ser 41:95–98
55. Huber T, Faulkner G, Hugenholtz P (2004) Bellerophon; a program to detect chimeric sequences in multiple sequence alignments. Bioinformatics 20:2317–2319
56. Castresana J (2000) Selection of conserved blocks from multiple alignments for their use in phylogenetic analysis. Mol Biol Evol 17:540–552
57. Librado P, Rozas J (2009) DnaSP v5: a software for comprehensive analysis of DNA polymorphism data. Bioinforma 25:1451–1452
58. Nei M (1987) Molecular evolutionary genetics. Columbia University Press, New York, 448
59. Templeton AR, Crandall KA, Sing CF (1992) A cladistic analysis of phenotypic associations with haplotypes inferred from restriction endonuclease mapping and DNA sequence data. III. Cladogram estimation. Genetics 132:619–633
60. Clement M, Posada D, Crandall KA (2000) TCS: a computer program to estimate gene genealogies. Mol Ecol 9(10):1657–1660
61. Schloss PD, Westcott SL, Ryabin T, Hall J, Hartmann M, Hollister EB, Lesniewski RA, Oakley BB, Parks DH, Robinson CJ, Sahl JW, Stres B, Thallinger GG, Van Horn DJ, Weber CF (2009) Introducing MOTHUR: open-source, platform-independent, community-supported software for describing and comparing microbial communities. Appl Env Microb 75(23):7537–7541
62. Smouse PE, Peakall R, Gonzales E (2008) A heterogeneity test for fine-scale genetic structure. Mol Ecol 17:3389–3400
63. Excoffier L, Smouse P, Quattro J (1992) Analysis of molecular variance inferred from metric distances among DNA haplotypes: application to human mitochondrial DNA restriction data. Genetics 131:479–491
64. Excoffier L, Laval G, Schneider S (2005) Arlequin (version 3.0): an integrated software package for population genetics data analysis. Evol Bioinform Online 1:47–50
65. Posada D (2008) jModelTest: phylogenetic model averaging. Mol Biol Evol 25(7):1253–1256
66. Akaike H (1974) A new look at the statistical model identification. IEEE Trans Autom Control AC-19:716–723
67. Tavaré S (1986) Some probabilistic and statistical problems in the analysis of DNA squences. Lect Math Life Sci 17:57–86
68. Hasegawa M, Kishino H, Saitou N (1991) On the maximum likelihood method in molecular phylogenetics. J Mol Evol 32 (5):443–445
69. Tamura K, Peterson D, Peterson N, Stecher G, Nei M, Kumar S (2011) MEGA 5: molecular evolutionary genetics analysis using maximum likelihood, evolutionary distance, and maximum parsimony methods. Mol Biol Evol. doi:10.1093/molbev/msr121
70. Yang Z, Rannala B (1997) Bayesian phylogenetic inference using DNA sequences: a Markov chain Monte Carlo method. Mol Biol Evol 14:717–724
71. Ronquist F, Huelsenbeck JP (2003) MRBAYES 3: Bayesian phylogenetic inference under mixed models. Bioinform 19:1572–1574
72. De los Ríos A, Ascaso C, Wierzchos J (1999) Study of lichens with different state of hydration by the combination of low temperature scanning electron and confocal laser scanning microscopies. Int Microb 2:251–257
73. Bergman B, Matveyev A, Rasmussen U (1996) Chemical signalling in cyanobacterial–plant symbioses. Trends Plant Sci 1:191–197
74. Rai AN, Söderbäck E, Bergman B (2000) Cyanobacterium–plant symbioses. Tansley review No 116. New Phytol 147:449–481
75. Svenning MM, Eriksson T, Rasmussen U (2005) Phylogeny of symbiotic cyanobacteria within the genus *Nostoc* based on 16S rDNA sequence analyses. Arch Microb 183:19–26
76. Bonnett HT, Silvester WB (1981) Specificity in the *Gunnera–Nostoc* endosymbiosis. New Phytol 89:121–128
77. Costa JL, Paulsrud P, Rikikinen J, Lindblad P (2001) Genetic diversity of *Nostoc* symbionts endophytically associated with two bryophyte species. Appl Env Microb 67:4393–4396
78. Paulsrud P, Lindblad P (1998) Sequence variation of the $tRNA^{leu}$ intron as a marker for genetic diversity and specificity of symbiotic cyanobacteria in some lichens. Appl Env Microb 64:310–315
79. Nilsson M, Bergman B, Rasmussen U (2000) Cyanobacterial diversity in geographically related and distant host plant of the genus *Gunnera*. Arch Microb 173:97–102
80. Meeks JC, Elhai J (2002) Regulation of cellular differentation in filamentous cyanobacterial in free-living and plant-associated symbiotic growth states. Microb Mol Rev 66:94–121
81. Rabassa J, Coronato A, Martínez Ó (2011) Late Cenozoic glaciatons in Patagonia and Tierra del fuego: an updated review. Biol J Linnean Soc 103:316–335
82. Nemergut DR, Anderson SP, Cleveland CC, Martin AP, Miller AE, Seimon A, Schmidt SK (2007) Microbial community succession in an unvegetated, recently deglaciated soil. M Ecol 53:110–122
83. Markgraf V, Huber UM (2010) Late and Postglacial vegetation and fire history in Southern Patagonia and Tierra del Fuego. Palaeogeogr Palaeoclim Palaeoecol 297:351–366

84. Gantar M, Kerby NW, Rowell P (1993) Colonization of wheat (*Triticum vulgare* L.) by N2-fixing cyanobacteria. III. The role of a hormogonia-promoting factor. New Phytol 124:505–513
85. Herdman M, Rippka R (1988) Cellular differentiation: hormogonia and baeocytes. Methods Enzymol 167:232–242
86. Martínez-Murcia AJ, Collins MD (1990) A phylogenetic analysis of the genus *Leuconostoc* based on reverse transcriptase sequencing on 16S rRNA. FEMS Microb Lett 70:73–83
87. Collins MD, Rodrigues U, Ash C, Aguirre M, Farrow JAE, Martínez-Murcia A, Phillips BA, Williams AM, Wallbanks S (1991) Phylogenetic analysis of the genus *Lactobacillus* and related lactic acid bacteria as determined by reverse transcriptase sequencing of 16S rRNA. FEMS Microbiol Lett 77:5–12
88. Amann RI, Lin C, Key R, Montgomery L, Stahl DA (1992) Diversity among *Fibrobacter* isolates: towards a phylogenetic classification. Syst Appl Microbiol 15:23–31
89. Fox GE, Wisotzeky JD, Jurtshuk P Jr (1992) How close is close: 16S rRNA sequence identity may not be sufficient to guarantee species identity. Int J Syst Bacteriol 42:166–170
90. Martínez-Murcia AJ, Benlloch S, Collins MD (1992) Phylogenetic interrelationships of the genera *Aeromonas* and *Pleisiomonas* as determined by 16S ribosomal DNA sequencing: lack of congruence with results of DNA-DNA hybridization. Int J Syst Bacteriol 50:412–421
91. Hart MW, Sunday J (2007) Things fall apart: biological species from unconnected parsimony networks. Biol Lett 3:509–512
92. Stackebrand E, Ebers J (2006) Taxonomic parameters revisited: tarnished gold standards. Microbiol Today 33:152–155
93. García-Martínez J, Acinas SG, Antón AI, Rodríguez-Valera F (1999) Use of the 16S–23S ribosomal genes spacer region in studies of prokaryotic diversity. J Microbiol Meths 36(1–2):55–64
94. Han D, Fan Y, Hu Z (2009) An evaluation of four phylogenetic markers in *Nostoc*: implications for cyanobacterial phylogenetic studies at the intrageneric level. Curr Microbiol 58:170–176
95. Silvester WB, McNamara PJ (1976) The infection process and ultrastructure of the *Gunnera–Nostoc* symbiosis. New Phytol 77:135–141
96. Towata EM (1985) Morphometric and cytochemical ultrastructural analyses of the *Gunnera kaalensis*/*Nostoc symbiosis*. Bot Gazzette 146(3):293–301